



**HAL**  
open science

## Evaluation of Timepix3 Si and CdTe Hybrid-Pixel Detectors' Spectrometric Performances on X- and Gamma-Rays

Guillaume Amoyal, Yves Ménesguen, Vincent Schoepff, Frédérick Carrel,  
Maugan Michel, Jean-Claude Angélique, Nicolas Blanc de Lanaute

► **To cite this version:**

Guillaume Amoyal, Yves Ménesguen, Vincent Schoepff, Frédérick Carrel, Maugan Michel, et al.. Evaluation of Timepix3 Si and CdTe Hybrid-Pixel Detectors' Spectrometric Performances on X- and Gamma-Rays. IEEE Transactions on Nuclear Science, 2021, 68 (2), pp.229-235. 10.1109/TNS.2020.3041831 . hal-03173799

**HAL Id: hal-03173799**

**<https://hal.science/hal-03173799>**

Submitted on 6 Apr 2021

**HAL** is a multi-disciplinary open access archive for the deposit and dissemination of scientific research documents, whether they are published or not. The documents may come from teaching and research institutions in France or abroad, or from public or private research centers.

L'archive ouverte pluridisciplinaire **HAL**, est destinée au dépôt et à la diffusion de documents scientifiques de niveau recherche, publiés ou non, émanant des établissements d'enseignement et de recherche français ou étrangers, des laboratoires publics ou privés.

# Evaluation of Timepix3 Si and CdTe hybrid-pixel detectors spectrometric performances on X- and gamma-rays

Guillaume Amoyal, Yves Menesguen, Vincent Schoepff, Frédérick Carrel, Maugan Michel, Jean-Claude Angélique, and Nicolas Blanc de Lanaute

**Abstract**— The Timepix3 hybrid-pixel readout chip consists of a matrix made of  $256 \times 256$  square-shaped pixels with a  $55 \mu\text{m}$ -pitch, which can be hybridized to several semiconductors, such as silicon (Si) or cadmium telluride (CdTe) with thicknesses up to 5 mm. Working as an event-based readout chip, it simultaneously records the Time-over-Threshold (ToT) in each pixel, measuring the deposited energy, as well as the Time-of-Arrival (ToA), with a time resolution of 1.5 ns.

In this paper, we present the energy calibration of two Timepix3 chips: the first one was bump-bonded with a  $300 \mu\text{m}$ -thick silicon sensor and the second one with a 1 mm-thick cadmium telluride sensor. Both detectors were calibrated with per pixel calibration, using the monochromatic SOURCE of Low-Energy X-rays (SOLEX from LNHB at CEA Saclay) and a set of calibration-grade sealed radioactive sources. Evaluations were carried out over the energy range of 6 keV – 122 keV for Timepix3 Si and 20 keV – 1.332 MeV for Timepix3 CdTe.

Based on this experimental procedure, an energy resolution of 2.6 keV (3.4 %) at 59.5 keV was observed for Timepix3 Si. For Timepix3 CdTe, this parameter was 5.6 keV (9.4 %) at 59.5 keV, 27.24 keV (4.1 %) at 661.7 keV, and 47.4 keV (3.5 %) at 1.332 MeV. It is the first time that CdTe bump-bonded Timepix3 spectral performances were evaluated for gamma-rays above 1 MeV. The reconstruction of the full-energy peak for such high energies is possible thanks to the ToA information, which allows the identification of all interactions caused by a given gamma-ray within the detector.

**Index Terms**—Timepix3, CdTe, Si, hybrid-pixel detector, spectrometric performances, X-rays, gamma-rays.

This paper was submitted August 6, 2020.

G. Amoyal, V. Schoepff, F. Carrel and M. Michel are with the CEA, LIST, Sensors and Electronics Architectures Laboratory, 91191 Gif-Sur-Yvette Cedex, France (e-mails: guillaume.amoyal@cea.fr, vincent.schoepff@cea.fr, frederick.carrel@cea.fr, maugan.michel@cea.fr).

Y. Menesguen is with CEA, LIST, Henri Becquerel National Laboratory (LNHB-LNE), 91191 Gif-Sur-Yvette Cedex, France (e-mail: yves.menesguen@cea.fr).

J.-C. Angélique is with Normandie Univ., ENSICAEN, UNICAEN, CNRS/IN2P3, LPC Caen, 14000 Caen, France (e-mail: angelique@lpccaen.in2p3.fr).

N. Blanc de Lanaute is with MIRION TECHNOLOGIES (CANBERRA) SAS, 6 Avenue du Vieil Etang 78180 Montigny-le-Bretonneux, France (e-mail: nblancdelanaute@mirion.com).

## I. INTRODUCTION

TIMEPIX3 is a hybrid-pixel readout chip developed, in 2013, within the framework of the Medipix3 international collaboration [1]. It is the successor of the Timepix [2] chip, as such, it can now record Time-Of-Arrival (ToA) and Time-Over-Threshold (ToT) simultaneously in each pixel. The chip is designed to work in data-driven mode, and can process a throughput up to 40 Mhits/cm<sup>2</sup>/s. The Timepix3 hybrid-pixel readout chip consists of a matrix made of  $256 \times 256$  square-shaped pixels with a  $55 \mu\text{m}$ -pitch. For each detected event, the ToA, with a time resolution of 1.5 ns, and the Time-over-Threshold (ToT) that gives access to deposited energy, are recorded. The Timepix3 chip can be hybridized to several semiconductors, such as silicon (Si) or cadmium telluride (CdTe) with thicknesses up to 5 mm.

In this paper, we present an experimental procedure for the energy calibration of Timepix3 with X-rays and gamma-rays. This enabled to evaluate the spectral performances of Timepix3. In this study, we considered a Timepix3 bump-bonded with a  $300 \mu\text{m}$ -thick silicon sensor, and a Timepix3 bump-bonded with a 1 mm-thick cadmium telluride sensor. Both detectors were calibrated using per pixel calibration using the SOURCE of Low-Energy X-rays (SOLEX from LNHB at CEA Saclay), and a set of standard radioactive sources. Evaluations were carried out over the 6 keV – 122 keV energy range for Timepix3 Si and from 15 keV – 1.3 MeV for Timepix3 CdTe.

Our future developments around Timepix3 are focused on achieving imaging spectrometry using coded-aperture and Compton imaging in the framework of gamma imaging for nuclear industry applications. Characteristic gamma-ray emitters in the nuclear industry are Am-241 (59.5 keV), Cs-137 (661.7 keV) and Co-60 (at 1.173 MeV and 1.332 MeV) [3]. Gamma-ray emitters sought to be located with gamma imaging techniques in the nuclear industry cover an energy from 59.5 keV (Am-241) up to 1.3 MeV (Co-60).

In this context, optimized energy calibration allows two things. On the one hand, it allows for better peak separation in a complex energy spectrum for coded-aperture imaging. On the other hand, this energy calibration improves Compton imaging performance, whether it would be in the case of a Compton imager based on a single Timepix3 CdTe, or of an imager based on Timepix3 Si as scatterer, combined with Timepix3 CdTe as absorber.

## II. MATERIALS & METHODS

### A. Experimental setup

For this study, a Timepix3 hybridized with a 300  $\mu\text{m}$ -thick P-on-N Si sensor and a Timepix3 hybridized with a 1 mm-thick N-on-P CdTe sensor equipped with Schottky contacts, were used. The first one was delivered by CERN, the second one by ADVACAM [4]. In order to simplify the terminology used in this paper, the term "Timepix3 Si" will refer to the Timepix3 detector hybridized to the silicon semiconductor, and "Timepix3 CdTe" will refer to the Timepix3 detector hybridized to the cadmium telluride semiconductor. The Timepix3 Si operates under hole collection with a 100 V bias voltage, whereas the Timepix3 CdTe operates under electron collection with a  $-300$  V bias voltage. These bias voltage values are those usually used for the detectors of the Medipix family [5]–[9].

Both Timepix3 detectors are controlled by the Katherine readout developed in cooperation between Faculty of Electrical Engineering, University of West Bohemia and IEAP, CTU [10]. A VHDCI cable allows communication between the Katherine readout and the Timepix3 detector. The Katherine readout also provides the bias for the Timepix3 detectors (power supply of the chip and bias of the semiconductor). The interface with the acquisition computer is carried out through an Ethernet cable.

The thresholds equalization is carried out prior to the energy calibration by means of the *Burdaman* software.

Fig. 1 illustrates the acquisition chain made of the Timepix3 detector, the Katherine readout system, and the acquisition computer. Fig. 2 presents a picture of the measurement setup.

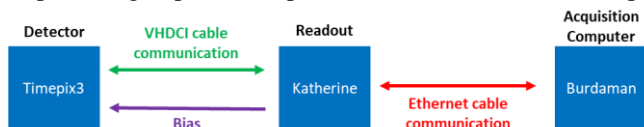


Fig. 1: Scheme of the three main blocks of the acquisition chain: the Timepix3 detector, Katherine readout, and the acquisition computer running the Burdaman software.

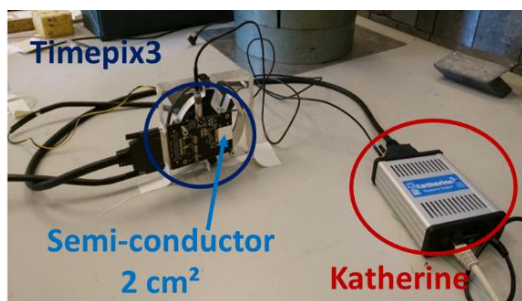


Fig. 2: Picture of a Timepix3 detector on its support, connected to the Katherine reading interface.

### B. Per pixel energy calibration

#### 1) Interests and motivation

In Timepix3, the energy deposited by a passing-through particle is measured using the Time-over-Threshold (ToT) method [11]. This method consists in measuring the time during which a pulse voltage is above a certain threshold. ToT values correspond to a number clock ticks during which the preamplifier output signal is over the threshold. The clock frequency for ToT value measurements is 40 MHz; therefore,

one ToT value corresponds to 25 ns. The objective of the energy calibration is to convert the ToT values to energy values. The Timepix3 detector consists of 65,536 pixels, each integrating a spectrometric measurement chain.

The measured raw ToT values for a given incident energy will be dispersed. This dispersion is induced on the one hand by the manufacturing process of the ASIC (Application Specified Integrated Circuit), which generates differences in the performances of transistors, and on the other hand, by the crystal defects of the CdTe sensor, such as dislocations and point defects, causing an inhomogeneous sensor layer [12], [13]. As an example, Fig. 3 shows the dispersion of ToT spectra for a set of 100 pixels, measured with Timepix3 Si exposed to an Am-241 source (59.5 keV gamma emission).

The interest of the per pixel energy calibration is to compensate the spread regarding the response of each individual pixel, and consequently, to correctly reconstruct energy deposited within the sensor.

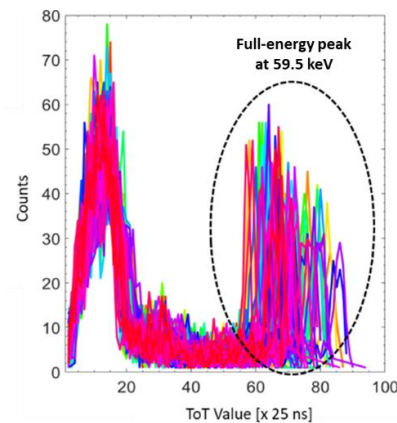


Fig. 3: ToT spectra of 100 Timepix3 Si pixels, exposed to an Am-241 source.

#### 2) Methods for energy calibration

For this study, we used the energy calibration curve proposed by Jakubek in [11] for the Timepix detector. The energy calibration curve for Timepix is described by (1), and illustrated in Fig. 4 [11]. In (1),  $E$  refers to the energy in [keV].

The energy calibration curve is composed of two parts: a linear part characterised by  $a$  and  $b$  parameters; and, a non-linear part characterised by  $c$  and  $t$  parameters, also described as "the knee". Since Timepix and Timepix3 work in a similar way, their energy calibration curves have the same shape. Hence, the procedure to determine their energy calibration curve is the same.

$$\text{ToT} = a \times E + b - \frac{c}{E-t}, \quad (1)$$

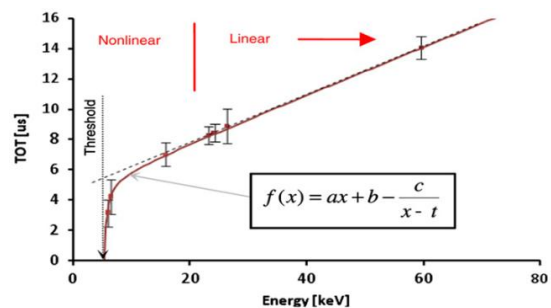


Fig. 4: Energy calibration curve for Timepix [11].

The per pixel energy calibration is obtained by analyzing ToT spectra measured for events that only interact within a single pixel, rejecting all events interacting in more than a single pixel. An energy calibration of each pixel implies that three main issues must be addressed which are described hereunder. First, it is important to have sufficient counting statistics in each pixel. Spectra of interest for energy calibration are those induced by a particle depositing its energy in a single pixel (55  $\mu\text{m}$ -pitch), which limits the photon energy range available for the energy calibration. Moreover, to simplify the analysis of the 65,536 ToT spectra, it is essential to have monoenergetic spectra.

In order to satisfy the constraints required by the per pixel energy calibration, we have used radioactive sources and X-ray fluorescence lines (XRF) as suggested in [11]. We also carried out measurement on the monochromatic source at SOLEX, described in paragraph 3).

### 3) SOLEX

The SOLEX (Source of Low Energy X-Rays) monochromatic tuneable X-ray photon source is located at the Henri Becquerel National Laboratory (LNHB), CEA LIST Paris-Saclay site. SOLEX produces X-ray photon beams over the 0.6 keV to 28 keV energy range, with a 0.1 % uncertainty on energy [14]. This facility is based on an X-ray tube, combined with a monochromating crystal, which allows an energy selection of the X-ray photons. The latter is carried out by the crystal, following Bragg's law, as in (2). In (2),  $d_{hkl}$  is the interreticular distance of the crystal,  $n$  is the order of reflection,  $\lambda$  is the wavelength of the incident X-ray photon,  $T$  is a correction term due to the reflection index, and  $\theta$  corresponds to the emission angle, also known as the Bragg angle. A drawing illustrating the key building blocks and a top view of the SOLEX facility are shown in Fig. 5.

$$n \times \lambda = 2 \times d_{hkl} \times (1 - T) \times \sin \theta, \quad (2)$$

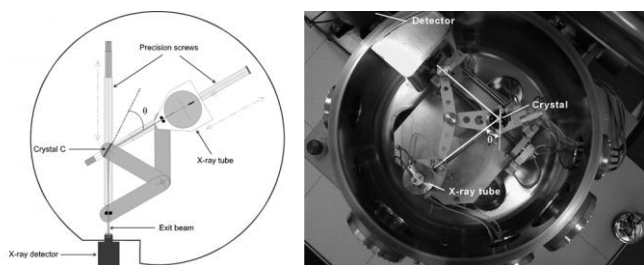


Fig. 5: Illustration of the SOLEX facility. On the left, scheme of the experimental SOLEX facility, with  $\theta$  the Bragg angle. On the right, top view of SOLEX.

### C. Evaluation of spectrometric performances

In order to evaluate the spectral performances of the calibrated Timepix3 detector, two criteria were used. The first criterion enables to evaluate the energy resolution as a function of the photon energy. The energy resolution is defined as the Full Width at Half Maximum (FWHM) of the considered peak's energy. Energy resolution values are fitted with the following formula [15], in which  $\Delta E$  is the FWHM of the considered peak's energy:

$$\frac{\Delta E}{E} = \frac{(a+b\sqrt{E+c \times E^2})}{E}, \quad (3)$$

The second criterion is the evaluation of the accuracy of the measured energy. It is evaluated by means of the relative error, defined by (4), with  $E_{theoretical}$  the theoretical energy, and  $E_{measured}$  the measured energy.

$$\varepsilon [\%] = 100 \times \frac{|E_{theoretical} - E_{measured}|}{E_{theoretical}}, \quad (4)$$

## III. ENERGY CALIBRATION AND SPECTROMETRIC PERFORMANCES OF TIMEPIX3 SI

### A. Per pixel energy calibration of Timepix3 Si

The per pixel energy calibration of the Timepix3 Si detector is obtained after processing SOLEX measurements, radioactive source measurements (Cs-137 (31.8 keV) source and Am-241 (59.5 keV) source), and XRF measurements (23.2 keV from the  $K_{\alpha 1}$  cadmium X-ray). Energies and emitting radionuclide used to evaluate the per pixel energy calibration curve of Timepix3 Si are summarized in Table I.

Using the method described in [11], the parameters of the energy calibration curve are determined as following:  $a$  and  $b$  are estimated using ToT measurements made for photons with an energy greater than 10 keV, while  $c$  and  $t$  parameters are estimated from ToT measurements of X-ray photons with an energy of 6 and 8 keV.

TABLE I  
ENERGIES AND EMITTING SOURCES USED TO DETERMINE THE PER PIXEL ENERGY CALIBRATION CURVE FOR TIMEPIX3 SI.

Sources	Energy [keV]
SOLEX	6; 9; 8; 10; 14
$K_{\alpha 1}$ Cd line	23.2
Am-241	59.5
Cs-137	31.8

The distribution of the calibration curves in energy per pixel of Timepix3 Si is shown in Fig. 6. This bidimensionnal graph describes the ToT value evolution as a function of energy for each pixel. The color scale corresponds to the pixel density, red corresponding to the most similar energy calibration curves, and blue corresponding to the most dissimilar energy calibration curves. The calibration curves, made of a linear and a non-linear part, is similar to the one found in the literature [11]. The overall detection threshold of Timepix3 Si is estimated from the distribution of the energy calibration curves per pixel (shown in Fig. 6). This detection threshold is 5 keV for the chip tested during our experiments.

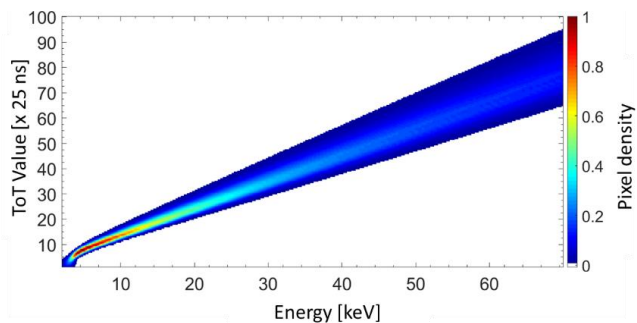


Fig. 6: Bidimensional histogram representing the distribution of the energy calibration curves per pixel of Timepix3 Si.

Per pixel energy calibration aims to compensate the spread in the response of each individual pixel to a calibrated photon energy. Fig. 7 shows Am-241 energy spectra for 100 pixels measured using Timepix3 Si, before and after energy calibration. In order to evaluate the benefit of the energy calibration, we determined the standard deviation of the centroid distribution of the full-energy peak at 59.5 keV. In this case, we considered the total single pixel spectra before and after energy calibration. Before calibration, the mean centroid distribution is 66.08 ToT with a resolving power in ToT value of 8.9 %. After energy calibration, the centroid is 59.47 keV, with a resolving power of 0.005 %.

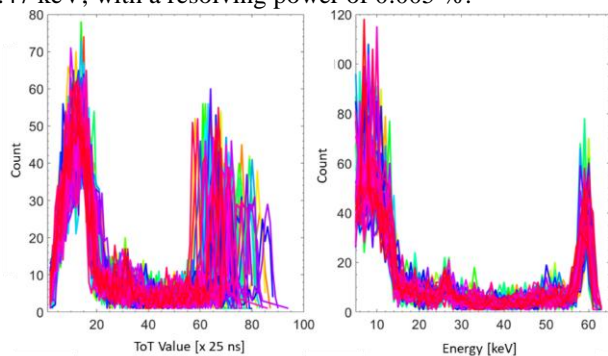


Fig. 7: Per pixel spectra (100 spectra displayed) measured with an Am-241 source and Timepix3 Si. On the left the per pixel ToT spectra, on the right the per pixel energy calibrated spectra.

Fig. 8 shows the ToT and energy calibrated spectra for a 1 MBq electrodeposited Am-241 source, placed at 20 cm from Timepix3 Si and for a live acquisition time of one hour. In Fig. 8, the full-energy peaks are distinguishable. The terms  $\mu$  and  $FWHM$  respectively are the mean energy and FWHM values of the considered peak. The energy conversion enables the identification of the full-energy peak of Am-241 characteristic gamma ray at 59.5 keV, and of the full-energy peak of the 26.8 keV gamma emission from Np-237 (daughter isotope of Am-241 following alpha decay) measured at 26.5 keV. The energy calibration also enables the identification of the strongest XRF photons of Np-237 at 13.8 keV and 17.9 keV [16].

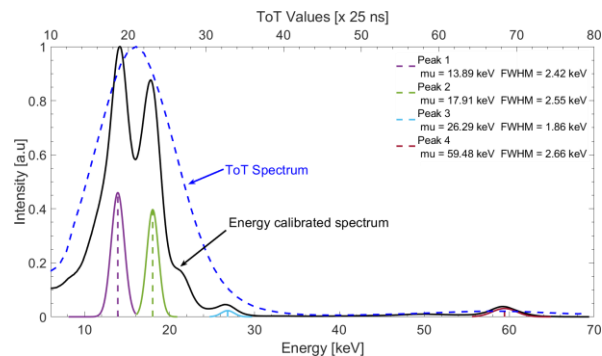


Fig. 8: ToT (blue dashed line) and energy calibrated spectrum (black solid line) of an electrodeposited Am-241 source with Timepix3 Si. The terms  $\mu$  and  $FWHM$  respectively are the mean energy and FWHM values of the peak under consideration.

### B. Evaluation of spectrometric performances of Timepix3 Si.

In order to estimate the Timepix3 Si detector spectrometric performances, additional measurements were carried out using radioactive sources from the laboratory, as well as using the SOLEX laboratory. The photon energies and the associated sources are listed in Table II. With Timepix3 Si, the evaluation of spectrometric performances is achieved on the 6 keV – 122 keV range. From those measurements, the evaluation of spectrometric performances of Timepix3 Si is carried out by determining either the energy resolution or the relative error (paragraph II.C), as a function of photon energy. Results are plotted in Fig. 9.

Experimental results show energy resolutions of 2.6 keV (3.4 %) at 59.5 keV and 5.8 keV (4.7 %) at 122.1 keV, and the relative error is lower than 2.5 % on an energy range from 6.4 keV to 122.1 keV, and lower than 0.5 % for incident energies greater than 25 keV.

TABLE II

LIST OF THE EMITTING SOURCES AND THEIR ASSOCIATED ENERGIES USED TO EVALUATE THE SPECTROMETRIC PERFORMANCES OF TIMEPIX3 Si.

Sources	Energy [keV]
Co-57	6.4; 14.4; 122.1; 136.5
SOLEX	8; 9; 10; 12; 14
Ba-133	81.0
Am-241	26.8; 59.5
Eu-152	40.1

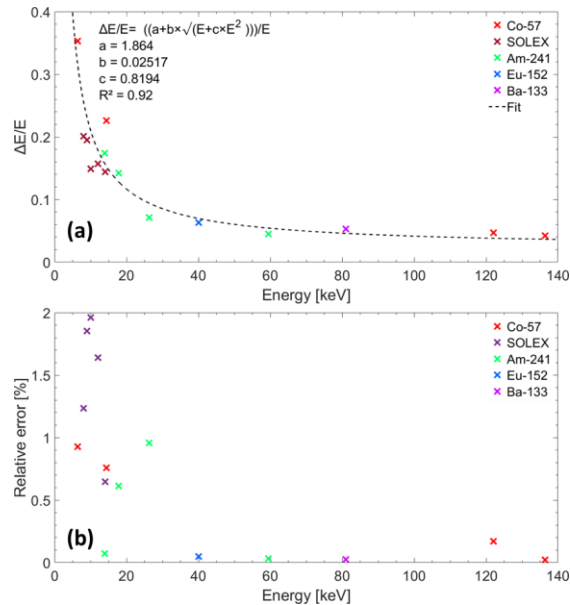


Fig. 9: Spectrometric performances of Timepix3 Si: (a) evolution of the energy resolution as a function of the photon energy; (b) evolution of the relative error as a function of the photon energy.

#### IV. ENERGY CALIBRATION AND SPECTROMETRIC PERFORMANCES OF TIMEPIX3 CdTE

##### A. Per pixel energy calibration of Timepix3 CdTe

In the case of Timepix3 CdTe, the energy calibration was evaluated by irradiating Timepix3 CdTe from the back of the detector, as suggested in [13]. This implies that before interacting in the semiconductor, incoming photons must pass through the PCB, but most importantly through the ASIC. Since the ASIC is mainly composed of silicon with a substantial thickness, it will filter “low-energy” photons. Therefore, the photon energies for the evaluation of the per pixel energy calibration curve of Timepix3 CdTe range from 25 keV to 81 keV. The origins and energies of the photons used to determine the per pixel energy calibration curve are listed in Table III.

In Table III, CdTe XRF are estimated close to 25 keV, this peak is composed of multiple emissions lines that are not separated, K shell lines from cadmium and telluride. K shell lines for cadmium and telluride are listed below:

- K shell lines from cadmium are described hereinafter  $K_{\alpha 1} = 23.17$  keV,  $K_{\alpha 2} = 22.98$  keV,  $K_{\beta 1} = 26.1$  keV and  $K_{\beta 3} = 26.06$  keV
- K shell lines from telluride are listed hereinafter  $K_{\alpha 1} = 27.47$  keV,  $K_{\alpha 2} = 27.2$  keV,  $K_{\beta 1} = 30.1$  keV, and  $K_{\beta 3} = 30.95$  keV.

Fig. 10 shows the bidimensionnal histogram describing the evolution of the linear portion of the calibration curve for each pixel of the ToT value as a function of energy. Since only the linear part of the energy calibration curve is determined, it was decided to set the overall detection threshold of Timepix3 CdTe at 15 keV, corresponding to a ToT value of 10.

TABLE III

ENERGIES AND EMITTING SOURCES OF PHOTONS USED TO EVALUATE THE PER PIXEL ENERGY CALIBRATION CURVE FOR TIMEPIX3 CdTE.

Sources	Energy [keV]
XRF CdTe	close to 25
Cs-137	31.8
Am-241	59.5
Ba-133	81.0

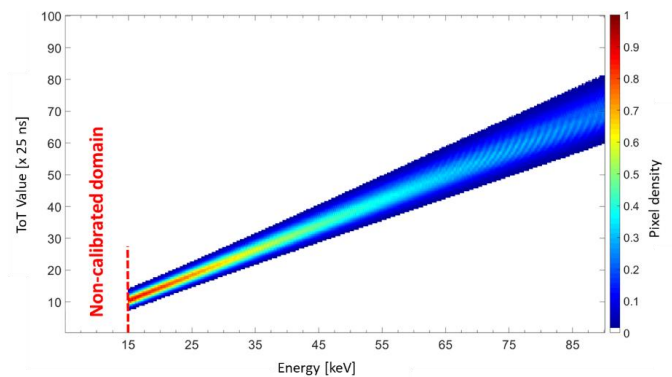


Fig. 10: Bidimensionnal histogram representing the distribution of the calibration curves in energy per pixel of Timepix3 CdTe.

Fig. 11 shows the spectra for 100 pixels before and after energy calibration, evaluated using an encapsulated Am-241 source. The centroid distribution of the per pixel spectra full-energy peaks before energy calibration has a mean value of 73.17 ToT and a standard deviation of 15.72 ToT. After energy calibration, this distribution has a mean value of 59.47 keV and a standard deviation of 0.1 keV. Similarly to the Timepix3 Si (paragraph III), the per pixel energy calibration allows to compensate the spread in the response of each individual pixel to a given energy. On the energy spectrum, the expected values (59.5 keV and 25 keV) described in Table III are reconstructed. The peak at 34.5 keV corresponds to the escape peak associated to the XRF of cadmium telluride.

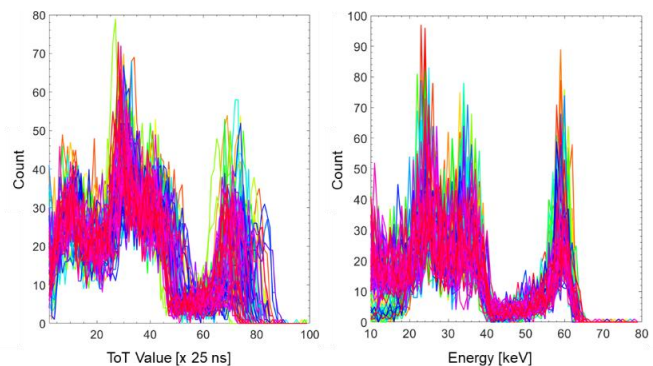


Fig. 11: Per pixel spectra (100 spectra displayed) of the measurement of an encapsulated Am-241 source using Timepix3 CdTe. On the left, the per pixel ToT spectra; on the right, the per pixel energy calibrated spectra.

### B. Evaluation of spectrometric performances of Timepix3 CdTe.

In a similar way to what has been proposed for Timepix3 Si, the spectrometric performances of Timepix3 CdTe are evaluated using the energy resolution and the relative error (paragraph III.B) as function of photon energy. The spectrometric performances of Timepix3 CdTe are evaluated on an energy range from 25 keV up to 1.33 MeV. Since the energy calibration was performed from the back of the sensor, the performances described hereafter are obtained by irradiating the sensor from the back. The emitting sources and photon energies used for this evaluation are listed in Table V. The density of the semiconductor material ( $Z$ ), as well as its thickness, make it possible to evaluate the spectrometric performances of Timepix3 CdTe over a wider energy range than Timepix3 Si.

TABLE IV

LIST OF THE EMITTING SOURCES AND THEIR ASSOCIATED ENERGIES USED TO EVALUATE THE SPECTROMETRIC PERFORMANCES OF TIMEPIX3 CdTe.

Sources	Energy [keV]
XRF CdTe	close to 25
Am-241	59.5
Co-57	122.1
Eu-152	40.1; 121.8; 244.7; 344.3 ; 1408
Ba-133	81.1; 356.0
Na-22	511.0
Cs-137	32.2; 661.7
Cs-134	569.3; 604.7; 795.9
Mn-54	834.8
Co-60	1173.2; 1332.5

Fig. 12 presents the measured energy spectrum of a Co-60 source and a Cs-137 facing the Timepix3 CdTe. Regions of interest of Cs-137 (661.7 keV) and Co-60 gamma emissions (1.173 MeV and 1.332 MeV) are highlighted. In contrast, measurement of Cs-137 and Co-60 sources were performed with a Timepix detector bump-bonded with a 1 mm thick CdTe semiconductor in [17]. With the current setup, the full energy peak of Cs-137 is reconstructed; however, it appears that the full energy peaks of Co-60 are not identified.

It is the ToA feature of Timepix3 that enables the coverage of such a wide energy range. For instance, for the Co-60 emissions, the Compton scattering probability of an incoming photon in a 1 mm thick CdTe material (2.8 % and 2.6 % respectively at 1.173 MeV and 1.332 MeV) dominates the photoelectric absorption probability by a factor of 20 (0.14 % and 0.11 % respectively at 1.173 MeV and 1.332 MeV). This difference in terms of probability implies that Co-60 gamma-rays will interact predominantly by Compton scattering. Without sufficient time sampling, it is not possible to distinguish photons interacting in the sensor in a short time frame.

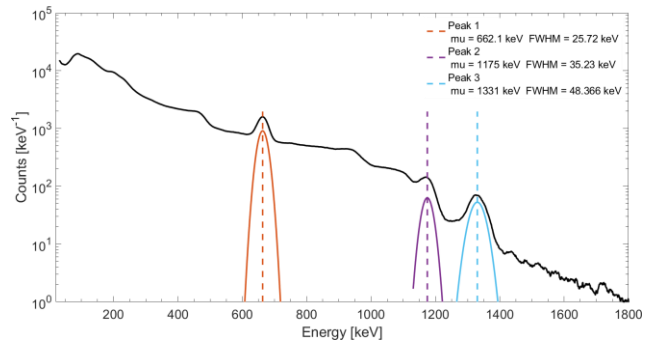


Fig. 12: The mean energy values of the full-energy peaks associated to each radioisotope are highlighted.

Energy resolution and the previously defined relative error are presented in Fig. 13 as a function of photon energy. With Timepix3 CdTe, the results show energy resolutions of 5.6 keV (9.5 %) at 59.5 keV, 27.2 keV (4.1 %) at 661.7 keV, 35.27 keV (3.0 %) at 1.17 MeV and 47.5 keV (3.6 %) at 1.33 MeV. The relative error is lower than 0.5 % for an incident energy greater than 15 keV.

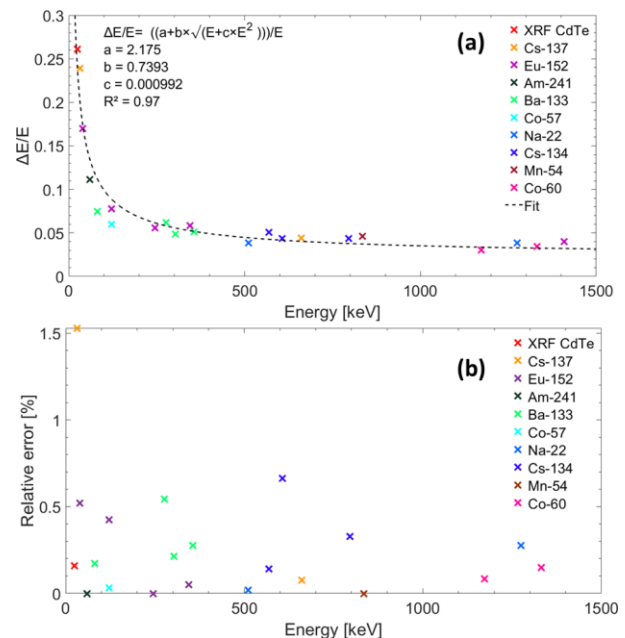


Fig. 13: Spectrometric performances of Timepix3 CdTe: (a) evolution of the energy resolution as a function of the photon energy, on the right; (b) evolution of the relative error as a function of the photon energy.

### V. CONCLUSION, DISCUSSION AND FUTURE DEVELOPMENTS

In this study, we have performed the per pixel energy calibration of two Timepix3 detectors: one hybridized with a 300  $\mu\text{m}$  thick silicon (Si) semiconductor, and one hybridized with a 1 mm thick cadmium telluride (CdTe) semiconductor. The energy calibration enabled us to define the energy thresholds of Timepix3 Si and Timepix3 CdTe respectively at 3.4 keV and 15 keV. Then, we evaluated the spectrometric performances of both detectors by means of the evolution of both the energy resolution and the relative error, as a function of the energy. The “knee-part” of the energy calibration curve for Timepix3 CdTe needs to be evaluated. This study should be the object of a future publication.

Energy resolving powers of Timepix3 Si and Timepix3 CdTe to commonly encountered energies in nuclear industry are presented in table v. In table v, energy resolving powers of other gamma imaging systems are also presented: WIX developed by CEA-IRFU, based on Caliste detector [18]; NuVISION, developed by NUVIA [19], and Polaris-H developed by H3D [20].

Compared to other existing gamma-ray spectro-imagers, energy measurements carried out with Timepix3 are not as resolved. The difference in resolving power is mainly due to the difference in semiconductor volume and pixel size. The pixel size of Timepix3 is 55  $\mu\text{m}$ -pitch, those of Caliste vary from 580  $\mu\text{m}$ -pitch to 1 mm-pitch, those of Polaris-H measure 1.72 mm-pitch, and those of NuVISION measure 2.5 mm-pitch. In the case of hybrid pixel detectors, the pixel size has a direct impact on the energy resolution: the larger the pixel size, the higher the energy resolution. Indeed, a smaller pixel size imply more charge sharing, which directly contributes to the deterioration of the energy resolution [21]. However, smaller pixels imply a better angular resolution regarding the capability of an imager based on Timepix3. Our future developments will concern the development and the evaluation of the performances of a hybrid gamma imager associating Compton and coded-aperture imaging techniques, based on Timepix3.

TABLE V  
ENERGY RESOLUTIONS OF SEVERAL GAMMA IMAGING SYSTEMS ON AN ENERGY RANGE FROM 59.5 KEV TO 1.33 MEV. (N.C: not communicated)

Energy [keV]	Energy resolving power [%]				
	WIX	NuVISION	Polaris-H	Timepix3	
				CdTe	Si
59.5	1.6	N.C	<5	9.5	3.4
81	N.C	N.C	<5	7.9	5.8
122	1.7	2.5	<5	6	4.7
662	1.01	1.5	0.86	4.5	
1173	2.1	N.C	< 1 %	3.0	
1333	6.3	N.C	< 1 %	3.4	

#### REFERENCES

- [1] "Medipix3 Collaboration," 2019. [Online]. Available: <https://medipix.web.cern.ch/>.
- [2] X. Llopart, R. Ballabriga, M. Campbell, L. Tlustos, and W. Wong, "Timepix, a 65k programmable pixel readout chip for arrival time, energy and/or photon counting measurements," *Nucl. Instruments Methods Phys. Res. Sect. A Accel. Spectrometers, Detect. Assoc. Equip.*, vol. 581, no. 1–2, pp. 485–494, 2007, doi: 10.1016/j.nima.2007.08.079.
- [3] International Atomic Energy Agency - IAEA, "Management of Disused Sealed Radioactive Sources - Nuclear Energy Series No. NW-T-1.3," 2014.
- [4] "ADVACAM," 2020. [Online]. Available: <http://advacam.com/>.
- [5] L. Tlustos, "Performance and limitations of high granularity single photon processing X-ray imaging detectors," PhD Thesis, Atominstitut der Österreichischen Universitäten, 2005.
- [6] D. Krapohl, C. Fröjd, E. Fröjd, D. Maneuski, H. Nilsson, and G. Thungström, "Investigation of charge collection in a CdTe-Timepix detector," *J. Instrum.*, vol. 8, no. 05, pp. C05003–C05003, 2013, doi: 10.1088/1748-0221/8/05/c05003.
- [7] E. Fröjd, "Hybrid pixel detectors," PhD Thesis, Mit Sweden University, 2015.
- [8] E. Fröjd *et al.*, "Timepix3: First measurements and characterization of a hybrid-pixel detector working in event driven mode," in *Journal of Instrumentation*, 2015, vol. 10, no. 1, pp. C01039–C01039, doi: 10.1088/1748-0221/10/01/C01039.
- [9] T. Billoud, C. Leroy, C. Papadatos, M. Pichotka, S. Pospisil, and J. S. Roux, "Characterization of a pixelated CdTe Timepix detector operated in ToT mode," *J. Instrum.*, vol. 12, no. 1, 2017, doi: 10.1088/1748-0221/12/01/P01018.
- [10] P. Burian, P. Broulím, M. Jára, V. Georgiev, and B. Bergmann, "Katherine: Ethernet Embedded Readout Interface for Timepix3," *J. Instrum.*, vol. 12, no. 11, pp. C11001–C11001, 2017, doi: 10.1088/1748-0221/12/11/c11001.
- [11] J. Jakubek, "Precise energy calibration of pixel detector working in time-over-threshold mode," *Nucl. Instruments Methods Phys. Res. Sect. A Accel. Spectrometers, Detect. Assoc. Equip.*, vol. 633, no. SUPPL. 1, pp. S262–S266, 2011, doi: 10.1016/j.nima.2010.06.183.
- [12] M. Fiederle *et al.*, "Comparison of CdTe, Cd<sub>0.9</sub>Zn<sub>0.1</sub>Te and CdTe<sub>0.9</sub>Se<sub>0.1</sub> crystals: application for  $\gamma$ - and X-ray detectors," *J. Cryst. Growth*, vol. 138, no. 1, pp. 529–533, 1994, doi: [https://doi.org/10.1016/0022-0248\(94\)90863-X](https://doi.org/10.1016/0022-0248(94)90863-X).
- [13] J. Fey, S. Procz, M. K. Schütz, and M. Fiederle, "Nuclear Inst. and Methods in Physics Research, A Investigations on performance and spectroscopic capabilities of a 3 mm CdTe Timepix detector," *Nucl. Inst. Methods Phys. Res. A*, vol. 977, no. June, p. 164308, 2020, doi: 10.1016/j.nima.2020.164308.
- [14] C. Bonnelle *et al.*, "SOLEX: a tunable monochromatic X-ray source in the 1–20keV energy range for metrology," *Nucl. Instruments Methods Phys. Res. Sect. A Accel. Spectrometers, Detect. Assoc. Equip.*, vol. 516, no. 2, pp. 594–601, 2004, doi: <https://doi.org/10.1016/j.nima.2003.09.031>.
- [15] J. F. Briesmeister, *MCNP – A General Monte Carlo N-Particle Transport Code*, no. March. 2000.
- [16] M. Rodrigues and M. Loidl, "L X-ray satellite effects on the determination of photon emission intensities of radionuclides," *Appl. Radiat. Isot.*, vol. 109, pp. 570–575, 2016, doi: 10.1016/j.apradiso.2015.11.100.
- [17] H. Lemaire *et al.*, "Implementation of an imaging spectrometer for localization and identification of radioactive sources," *Nucl. Instruments Methods Phys. Res. Sect. A Accel. Spectrometers, Detect. Assoc. Equip.*, vol. 763, pp. 97–103, 2014, doi: 10.1016/j.nima.2014.05.118.
- [18] D. Maier *et al.*, "Second generation of portable gamma camera based on Caliste CdTe hybrid technology," *Nucl. Instruments Methods Phys. Res. Sect. A Accel. Spectrometers, Detect. Assoc. Equip.*, vol. 912, 2018, doi: 10.1016/j.nima.2017.12.027.

- [19] G. Montemont *et al.*, “NuVISION: A Portable Multimode Gamma Camera based on HiSPECT Imaging Module,” *2017 IEEE Nucl. Sci. Symp. Med. Imaging Conf. NSS/MIC 2017 - Conf. Proc.*, pp. 6–8, 2018, doi: 10.1109/NSSMIC.2017.8532713.
- [20] C. G. Wahl *et al.*, “The Polaris-H imaging spectrometer,” *Nucl. Instruments Methods Phys. Res. Sect. A Accel. Spectrometers, Detect. Assoc. Equip.*, 2014, doi: 10.1016/j.nima.2014.12.110.
- [21] D. Vavrik *et al.*, “Modular pixelated detector system with the spectroscopic capability and fast parallel read-out,” *J. Instrum.*, vol. 9, no. 06, pp. C06006–C06006, 2014, doi: 10.1088/1748-0221/9/06/c06006.